# Demethylzeylasteral (T-96) Initiates Extrinsic Apoptosis Against Prostate Cancer cells by Inducing ROS-Mediated ER Stress and Suppressing Autophagic Flux

**Dong-Lin Yang** ( dlyang@cqwu.edu.cn )
Chongqing University of Arts and Sciences https://orcid.org/0000-0002-1768-8644
**Ya-jun Zhang**
Chongqing University of Arts and Sciences
**Liu-jun He**
Chongqing University of Arts and Sciences
**Chun-sheng Hu**
Chongqing University of Arts and Sciences
**Li-xia Gao**
Chongqing University of Arts and Sciences
**Jiu-hong Huang**
Chongqing University of Arts and Sciences
**Yan Tang**
Chongqing University of Arts and Sciences
**Jie Luo**
Chongqing University of Arts and Sciences
**Dian-yong Tang**
Chongqing University of Arts and Sciences
**Zhong-zhu Chen**
Chongqing University of Arts and Sciences

**Research Article**

**Keywords:** T-96, CaP, ER stress, apoptosis, autophagic flux, cisplatin

**Posted Date:** March 13th, 2021

**DOI:** https://doi.org/10.21203/rs.3.rs-298068/v1

# Abstract

Demethylzeylasteral (T-96), a pharmacologically active triterpenoid monomer extracted from Tripterygiumwilfordii Hook F (TWHF), has been reported to exhibit anti-neoplastic effect on several types of cancer cells. However,whether it has the anti-tumour capability in human Prostate cancer (CaP)cells and what's the precise regulatory mechanisms underlying the anti-proliferation effect of T-96 on human CaP. In the current study, T-96 exerted significant cytotoxicity to CaP cells in vitro and induced cell cycle arrest at S-phase in a dose-dependent manner. Furthermore, mechanistic investigation indicated that through inducing endoplasmic reticulum (ER) stress caused by intracellular accumulation of reactive oxygen species (ROS), T-96 significantly promoted autophagy initiation while blocked the autophagic flux and finally caused extrinsic apoptosis in CaP cells, implying that ER stress induced byT-96 initiated caspase dependent apoptosis to inhibit CaP cells. Moreover, as a novel lethal ER stress inducer, T-96 was capable to enhance the sensitivity of CaP cells to chemotherapeutic drug cisplatin. Taken together, our data implied that T-96 is a novel ER stress and autophagy modulator, and has the potential applications for CaP therapy in clinic.


# Introduction

Prostate cancer (CaP) is one of the most common and lethal malignancies in men across the worldwide threating the males' health[1]. Increasing researches show that CaP is resulted from the androgen receptor (AR), which is a ligand-dependent transcription factor and belongs to the nuclear receptor family[2, 3]. Currently, the main treatment for early stage of CaP is the androgen deprivation due to the dependence on androgens for initial CaP cell proliferation, while the standard therapies related to castration-resistant CaP, a lethal form which has no effective therapy to date, contains hormone therapy, chemotherapy and radiation because of the emergence of androgen-independence[4]. Unfortunately, despite enormous advances in these treatments, the incidence of CaP is still augmenting because of a preference of recurrence and metastasis[5]. Thus, identifying novel agents for efficacious CaP suppression, without significant side influence, is highly desired to improve survival rates among CaP patients.

The endoplasmic reticulum (ER) is the largest intracellular organelle and plays a vital role in synthesis, modification, assembly, folding and structural maturation of proteins[6]. In the ER lumen, abundant accumulation of unfolded or misfolded proteins attributed to excess of ER protein-folding capability can lead to occurrence of ER stress[7, 8]. In order to recover the homeostasis of ER when ER stress happens, cells have evolved a highly protective transduction signal pathway, which is referred as unfolded protein response (UPR) to alleviate ER stress by enhancing protein folding ability, reducing protein transduction rate and degrading unfolded and misfolded proteins[9, 10]. ER stress can trigger autophagy in damaged cells by inducing UPR, contributing the impaired ER engulfed by the autophagic vesicles. The UPR signal is mainly initiated by activation of three transmembrane proteins located on ER: IRE1α (Inositol-requiring enzyme 1α), PERK (Double-stranded RNA-dependent protein kinase (PKR)-like endoplasmic reticulum kinase) and ATF6 (Activating transcription factor 6)[11, 12]. It is an attempt to help the stressed cells

accommodate and survive from ER stress process by transcriptional and translational reprogramming[13]. However, in the event of that protein folding homeostasis cannot be remediated in ER, the UPR converts into an alternative signaling platform termed terminal UPR which eventually promotes apoptosis due to toxicity of unfolded/misfolded proteins[9, 10, 14]. Therefore, ER stress accumulation overwhelming a critical threshold induced by novel compounds and subsequently induction of programmed cell death signalling pathway may be an effective strategy for cancer therapy

*Tripterygiumwilfordii* Hook F (TWHF), commonly known as “ lei gong teng ” or “ thunder god vine”, has been reported to treat a wide range of autoimmune and inflammatory diseases such as rheumatoid arthritis, ankylosing spondylitis, systemic lupus erythematosus and psoriasis[15–18].The major effective components of TWHF consist of triptolide and celastrol, which are diterpenoid and triterpenoid extracts. The active ingredient extracts of TWHF including triptolide and celastrol have been proved to play anti-tumourabilities by inducing apoptotic or autophagic cell death or cell cycle arrest in a series of cancer cells[17–22]. Demethylzeylasteral (T-96), a triterpenoid monomer compound, is isolated from the TWHF and exerts considerably lower toxicity in comparison with other bioactive compounds *in vitro* cytotoxicity or *in vivo* toxicity, including triptonide, celastrol and triptolide[23]. Previous studies have indicated that T-96 is capable to suppress cell proliferation, metastasis and angiogenesis, and to promote cell apoptosis in various malignant carcinomas, such as melanoma[24], glioblastoma[25] and breast cancer[26]. Interestingly, T-96 is also involved in the proliferation inhibition of pancreatic cancer through autophagy-induced apoptosis, and significantly increases chemosensitivity to gemcitabine[27]. However, to date, no study has yet been performed to investigate the regulatory mechanisms underlying the anti-tumour effects of T-96 in human CaP.

In the present study, we evaluated the anti-tumour effects of T-96 against CaP and their underlying mechanisms associated with the inhibition capability to CaP cell growth. We further investigated whetherT-96could increase the chemo-sensitivity to cisplatin. Our results demonstrated for the first time that T-96 mainly exerted proliferation inhibition through cell cycle arrest, initiating autophagy and inducing apoptotic cell death mediated by ER stress. Additionally, T-96 had the ability to increase CaP cells’ chemo-sensitivity to cisplatin through regulating the crosstalk between apoptotic cell death and ER stress.

## Materials And Methods

# Reagents and antibodies

Demethylzeylasteral (T-96, molecular formula: C29H36O6, molecular weight: 480, T3418), Z-VAD-FMK (T6013), Rapamycin (T1537), Chloroquine (T8689) and Cisplatin (T1564) were purchased from TOPSCIENCE (Shanghai, China).The reagents including 3-(4,5-Dimethylthiazol-2-yl)-2,5-diphenyltetrazolium bromide (MTT), Penicillin-Streptomycin, propidium iodide (PI) were purchased from Sigma-Aldrich (MO, USA).Cell culture medium including DMEM (SH30022.01B) and F12K (SH30526.01) were ordered from HyClone (Logan, USA) while fetal bovine serum (FBS) was purchased from Natocor

(Cordoba, Argentina). All the primary antibodies involved in present study were bought from Cell Signaling Technology (MA, USA) and the secondary antibodies were purchased from LI-COR Biosciences (NE, USA).

# Cell culture

Human CaP cell lines DU145 and PC3 were obtained from the American Type Culture Collection (ATCC, VA, USA). Both cell lines were mycoplasma-free and have been authenticated using STR profiling. Cells were cultured in DMEM/HIGH glucose culture medium and F12K supplemented with 10% fetal bovine serum, 1%Penicillin-Streptomycin at 37 °C in a humidified incubator containing 5% $CO_2$.

# Cell viability assay

DU145 and PC3 cells were plated into 96-well plates (3000 cells/well) and incubated with various concentrations of T-96, cisplatin, T96 and cisplatin for designed times at 37 °C. Then, 1% MTT was added (20 μL/well) and incubated at 37 °C for 4 h. After the crystals dissolution in DMSO, the absorbance value at 570 nm was detected in a microplate reader (Bio-Tek, VT, USA), and analyzed by GraphPad Prism 7.0. All experiments were performed in triplicates independently.

# Colony formation assay

DU145 and PC3 cells were plated into six-well plates (500 cells/well) and cultured for 7 days under designed drug conditions. Colonies were washed twice with PBS (Phosphate Buffered Saline), fixed with 4% PFA (Paraformaldehyde) for 15 min at room temperature and then stained with 1% crystal violet for 30 min. All statistical measurements were performed in triplicates independently.

# 5-Ethynyl-20-deoxyuridine (EdU) incorporation assay

Proliferation of human CaP cells was investigated using BeyoClick™ EdU Cell Proliferation Kit with Alexa Fluor 555 (C0075S, Beyotime, Shanghai, China) according to the manufacturer's protocols. Briefly, logarithmic growth stage cells were seeded into 24-well plate prior to treatment with different concentrations of T-96 for 48 h. DU145 and PC3 cells were incubated with 10μMEdU working solution in the dark room for 2 h at 37°C. Next, the labeled cells were fixed with 4% PFA for 20 min, permeabilized with 0.1% Triton-X100 for 10 min,and then stained with click reaction solution in the dark room for 30min. In addition, cells were incubated with 1 mg/mL DAPI-PBS for 30 min. The images were captured with fluorescence microscope (Olympus, Tokyo, Japan)and the percentage of EdU-positive cells was calculatedby GraphPad Prism 7.0.

# Flow cytometry analysis

DU145 and PC3 cells during the logarithmic growth phase were harvested and transferred into six-well plates with 30% cell density. After exposure to the indicated concentrations of T-96, Z-VAD-FMK, T-96 and Z-VAD-FMK, rapamycin, T-96 and rapamycin, chloroquine, T-96 and chloroquine, cisplatin, and T-96 and cisplatin for 48 h respectively, cells were collected and employed in flow cytometry analysis. For cell cycle assay, cells were harvested, fixed with 70% ethanol in 4 °C for 24 h, and then washed three times with PBS. Subsequently, PBS containing 50μg/ml PI and 100μmg/ml RNase (Sigma Aldrich, USA) were added to the cells for 0.5 h incubation at 37 °C. Finally, the stained cells were analyzed using BD AccuriTM C6 flow cytometry (BD Biosciences, USA) and FlowJo 7.6 software. For cell apoptosis assay, the collected cells were subjected to an AnnexinV-FITC/PI apoptosis assay kit (C1062S, Beyotime, China) according to the manufacturer's protocols. The fluorescence-positive cells were analyzed using a flow cytometer within 1 h to assess the proportion of apoptotic cells, and the apoptotic rate was visualized using FlowJo 7.6.

# Western blotting analysis

The harvested DU145 and PC3 cells were lysed in RIPA buffer (P0013B, Beyotime, Shanghai, China) supplemented with protease and phosphatase inhibitor cocktail (P1046, Beyotime, Shanghai, China) at 4 °C for 30 min, and then the protein concentration was quantified using a BCA Protein Assay Kit (P0010S, Beyotime, Shanghai, China). Protein lysates (30 μg/lane) were loaded on appropriate SDS gels, resolved by electrophoresis and transferred to PVDF membranes (IPVH00010, Millipore, Billerica, MA, USA). After incubation with 5% BSA in TBST for 2 h at room temperature, the membranes were incubated with the indicated primary antibodies overnight at 4 °C. Subsequently, the membranes were incubated with the corresponding IRDye 800CW donkey anti-mouse IgG (H + L) or IRDye 680LT donkey anti-rabbit IgG (H + L) secondary antibody, and immunoreactivity was visualized by an odyssey two-color infrared fluorescence imaging system (LI-COR Biosciences, NE, USA). b-tubulin was used as the loading control.

# Determination of reactive oxygen species (ROS) formation

Intracellular ROS level was measured using a ROS Assay Kit (S0033S, Beyotime, Shanghai, China) according to the manufacturer's protocols. Briefly, after treatment with or withoutT-96, the collected CaP cells were incubated with serum-free DMEM or F12K containing DCFH-DA (10 μM) for 20 min. Subsequently, cell suspensions were centrifuged and washed three times with serum-free DMEM, and then visualized by a fluorescence microscope (IX53/DP80, Olympus Corporation, Japan).

# $Ca^{2+}$ signals measurement

The signals of intracellular $Ca^{2+}$were determined with Fluo-4 AM (S1060, Beyotime, Shanghai, China) according to manufacturers' protocols. Briefly, CaP cells were collected and washed three times with PBS,

and then incubated with 1 μMFluo-4 AM in PBS for 30 min at 37 °C. Next, cells loading with Fluo-4 AM were washed with PBS and incubated for an additional 20 min to ensure that Fluo-4 AM was completely transformed into Fluo-4.The fluorescent intensity was captured by a fluorescence microscope (IX53/DP80, Olympus Corporation, Japan).

# Autophagy analysis

For autophagy analysis, DU145 and PC3 cells stably expressed GFP-LC3B and mCherry-EGFP-LC3B via a lentivirus infection process were used. In brief, the lentivirus packaging vectors (Pspax2, pMD2G) and GFP-LC3B/mCherry-GFP-LC3B were co-transfected into HEK293T cells by the Lipo8000 transfection reagent (C0533,Beyotime, Shanghai, China) according to the manufacturer's protocols. Viral particles were collected after 48 h transfection and then infected into the CaP cells in the assistance of Polybrene (10 μg/mL). Subsequently, cells were screened with puromycin (10 μg/mL) to obtain the stable cells expressing GFP-LC3B or mcherry-EGFP-LC3B. After treatment with designed concentrations of T-96, the transgenic cells were analyzed using the high content analysis system-operetta CLS$^{TM}$ (PerkinElmer, Waltham, MA, USA).

# Statistical analysis

All experiments were performed in triplicates independently. GraphPad Prism version 7.0 (GraphPad Software, San Diego, CA, USA) was used for the statistical analysis. Data are presented as the mean ±Standard deviation, and the ANOVA method was used to compare differences between groups. $P<0.05$ was considered to indicate a statistically significant difference.

## Results

# Cytotoxicity of T-96on CaP cells

As T-96 has capability to suppress cancer cell growth, we investigated whether it can play anti-cancer effect on CaP cells such as DU145 and PC3. The chemical structure was indicated in Fig. 1A. The results showed that T-96 can significantly inhibit cell proliferation in growth curve in a dose- and time-dependent manner (Fig. 1B). The half maximal inhibitory concentration ($IC_{50}$) values of T-96 in DU145 and PC3 were 11.47 μM and 13.10μM, respectively (Fig. 1C). Additionally, DU145 and PC3 cells exposed to T-96 exhibited dramatic cell number decrease with consistent concentration increase (Fig. 1D). To further evaluate the inhibition of T-96 to CaP cell, colony formation and 5-Ethynyl-2'-deoxyuridine (EdU) assays were used to investigate cell growth and proliferation. As shown in Fig. 1E, colony formation assay showed that CaP cells exposed to T-96 exhibited the smaller and decreased colony numbers in a dose-dependent manner compared with the control group. Consistently, in comparison with the untreated

group, EdU-staining indicated that DNA synthesis was considerably decreased in a dose-dependent manner following exposure to T-96, implying its survival and growth inhibition effect on CaP (Fig. 2A).

T-96inhibited cell cycle procession by arresting CaP cells into S-phase

To deeply investigate the mechanism underlying antiproliferation effect of T-96 on CaP, cell cycle analysis was conducted in CaPcells after treatment with or without T-96. As indicated in Fig. 2B, the result of flow cytometry showed that T-96could dramatically arrest cell cycle at S-phase through decreasing the distribution of G0/G1 phase in both DU145 and PC3 cells. Since the effect of T-96 on cell cycle arrest in DU145 and PC3 cells was determined, its effect on the expression levels of S-phase related proteins was further examined to confirm the regulatory role in cell cycle distribution. As shown in Fig. 2C, western blotting showed that T-96 significantly decreased the levels of CyclinA, Cyclin B, CDK1 and CDK2, while P21 and P27 were considerably increased following exposure to T-96 in a dose dependent manner in DU145 and PC3 cell lines. Taken together, these dada demonstrated that T-96 may inhibit cell proliferation by inducing S-phase cell cycle arrest in CaP cells.

# T-96 Induced Extrinsic -apoptosis Signalling Pathway In Cap Cells

To gain more insights into the mode of T-96-induced proliferation suppression in CaP cells, an Annexin V-FITC/PI assay was conducted by flow cytometry after exposure to T-96 for 48h. As indicated in Fig. 3A, flow cytometry analysis showed that T-96 could significantly induce cell apoptosis in CaP cells and increase the proportion of late-phase apoptosis (from 5.47–32..5% for DU145 cells, $p < 0.001$; from 3.03–33.8% for PC3 cells, $p < 0.001$) in a dose-dependent manner. To further determine whether T-96 can induce the extrinsic-apoptosis signaling pathway in response to T-96 treatment, we detected the protein levels related to this pathway. Consistently, compared with the control group, T-96 treatment led to an obvious increase of Cleaved Caspase8 (C-Cas8), Cleaved Caspase3 (C-Cas3) and Cleaved PARP in a dose-dependent manner (Fig. 3B). Moreover, a specific caspase3 inhibitor, Z-VAD-FMK, considerably decreased the apoptotic rate in both DU145 and PC3 cells, suggesting Z-VAD-FMK could partially rescue cell apoptosis induced by T-96 (Fig. 3C). In summary, these data indicated that apoptotic effect of T-96 depended on the activation of apoptosis-related proteins through external apoptotic pathway in CaP.

# T-96 induced Er Stress By Generating Ros In Prostate Cells

Previous studies have revealed that ROS is involved in ER stress and cell death [28–30]. In order to investigate whether T-96 could induce the generation of ROS, intracellular ROS generation was measured by fluorescence microcopy after incubation with the specific ROS-detecting fluorescent dye, 2',7'-dichlorofluorescein diacetate (DCF-DA) in DU145 and PC3 cells. As showed in Fig. 4A, ROS was significantly produced after treatment with different concentrations of T-96 when compared with the control group. Consistently, the expression of oxidative stress responsive gene, nuclear factor-like 2

(NRF2), was enhanced after exposure to T-96 in a dose dependent manner, suggesting the excessive ROS accumulation within CaP cells (Fig. 4C). Furthermore, we evaluated whether T-96 could promote ER stress through accumulation of excessive intracellular ROS. Since the accumulation of polyubiquitinated proteins is one of the most important symbol of ER stress, we evaluated whether T-96 can influence the level of total polyubiquitinated proteins was detected in both DU145 and PC3 cell lines using western blotting. As shown in Fig. 4B, T-96 resulted in a remarkable increase of polyubiquitinated protein levels in a dose-dependent manner in both DU145 and PC3 cells. To alleviate the accumulation of misfolded and unfolded proteins, stressed cells may initiate a homeostatic intracellular signaling pathway cumulatively, the UPR, to recover the ER function by increasing protein folding ability and degrading the accumulated proteins[9, 10, 31]. As is expected, PERK phosphorylation was increased and the protein levels of several UPR associated proteins, such as BIP, IRE1α, Ero1-L1α and PDI, were remarkably up-regulated in a dose-dependent manner after T-96 treatment (Fig. 4C). Additionally, ER stress is coupled with alteration in $Ca^{2+}$ homeostasis which in turn contributes to ER stress and apoptotic cell death[32]. Next, we evaluated whether T-96 could disturb the $Ca^{2+}$ homeostasis. A $Ca^{2+}$ specific indicator Furo-4/AM was employed to stain the CaP cells after challenging with different concentrations of T-96. Interestingly, T-96 considerably led to the intracellular fluorescence accumulation, suggesting ER stress induction and $Ca^{2+}$ release to cytoplasm from ER when treatment with this compound (Fig. 4D). In summary, these results demonstrated that T-96 induced ROS generation, which further initiated the ER stress and subsequent the intracellular $Ca^{2+}$accumulation.

T-96 initiated autophagy while blocked autophagic flux and subsequently induced apoptosis

Several studies have demonstrated that ER stress could promote autophagy activation to swallow stressed ER by forming autophagosome[33, 11, 12]. We investigated whether autophagy was regulated after treatment with T-96. The autophagy induction in response to T-96 in CaP cells can be detected by the appearance of punctate LC3 signals using immunofluorescence, or by the LC3-II/LC3-I converted ratio using western blotting. Based on these, we first used DU145 and PC3 cells transiently transfected with GFP-tagged LC3 to demonstrate the autophagy regulatory effect of T-96. Of note, T-96 dramatically induced an accumulation of GFP-LC3 puncta, representing the number of autophagic vacuoles, and LC3-II conversion was largely increased in a dose-dependent manner in both DU145 and PC3 cells (Fig. 5A and 5B). Adenosine monophosphate-activated protein kinase (AMPK), mammalian target of rapamycin (mTOR)and mitogen-activated protein kinases (MAPK/ERK) signaling pathways are three mainautophagy-regulating pathways[34, 35]. We explored whether AMPK, mTOR and MAPK/ERK were involved in autophagy initiation process in response toT-96. As expected, the phosphorylation levels of AMPK and MAPK/ERK were significantly enhanced in dose-dependent manner, while the phosphorylation level of mTOR was reduced in CaP cells (Fig. 5B). Accumulating evidence also indicated that drug-mediated activation of MAPK/ERK can impair autophagy maturation by disrupting the fusion between autophagosome and lysosome[36, 37].To further determine whether T-96 is capable to modulate the progression of autophagic flux, double tagged mCherry-GFP-LC3B reporter, which is pH sensitive, was transfected into CaP cells to evaluate the fusion efficiency of autophagosome and lysosome. The yellow

fluorescent represented the number of non-acidic autophagosomes, whereas the red fluorescent labeled autolysosomes. As shown in Fig. 5C, a remarkable increase in the number of yellow fluorescent vesicles of both DU145 and PC3 cells exposed to T-96 was observed as compared with control after 12h treatment, implying that apoptotic flux was perturbed due to a defect of fusion between autophagosome and lysosome. It has been previously reported that initiation of ER stress induced by accumulation of polyubquitinated proteins due to apoptotic flux blockage were involved in the apoptosis induction [9, 10, 14, 28–30]. Consistently, the combination of T-96 with rapamycin, an inhibitor of mTOR, could slightly increase apoptosis compared with T-96 treatment alone. In comparison, the apoptosis was significantly promoted in CaP cells when combining T-96 with chloroquine, an autophagic flux inhibitor that decreases autophagosome–lysosome fusion, implying that autophagic flux blockage can enhance apoptosis-promoting activity of T-96 (Fig. 5D). Taken together, these results revealed that T-96 initiates autophagy whereas suppresses autophagic flux, which contributes to apoptosis in both DU145 and PC3 cells.

T-96 enhancedCaP cells' sensitivity to cisplatin through ER stress and apoptosis

Accumulating studies have demonstrated that autophagy induced by chemotherapy or radiotherapy may protect cancer cells from apoptosis due to generation of resistance while the suppression of autophagic flux can improve cells' sensitivity to chemotherapy because of cell death induction[38–40]. As an autophagy modulator, we therefore explored whether T-96 could improve the sensitivity of CaP cells to chemotherapy drugs, T-96 alone or T-96 in combination with an antineoplastic chemotherapy agent, cisplatin, was used to treat CaP cells. To examine the growth-inhibitory effect of T-96 and cisplatin co-treatment on CaP cells, both DU145 and PC3 cells were exposed to various concentrations of T-96 (0, 8, and 16 μM) and cisplatin (0, 1.25, 2.5, 5, 10 and 20μM) alone or in combination for 48 h.MTT assay showed that co-treatment of DU145 and PC3 cells with T-96 and cisplatin led to obvious increase in suppressing cell proliferation, whereas lower cytotoxicity was detected when monotherapy was given (Fig. 6A). Next, we evaluated the apoptosis induction after co-treatment CaP cells with T-96 and cisplatin, and found that combined treatment caused a higher apoptotic rate than that of monotherapy (Fig. 6B). Consistently, western blotting showed that T-96 and cisplatin co-treatment resulted in the increase of C-Cas3 and PARP relative to the levels under single cisplatin treatment (Fig. 6C). Subsequently, NRF2 and the UPR associated proteins, such as p-PERK, BIP, IRE1α, Ero1-L1α and PDI were up-regulated under T-96 and cisplatin combination treatment compared to the expression under single-agent treatment alone, indicating that co-treatment was more effective in initiating oxidative stress response and UPR (Fig. 6D). Taken together, these results suggested that T-96 was capable to improve the chemosensitivity of CaP cells to cisplatin.

# Discussion

Although achieved dramatic advances in CaP therapies, it exerts an unfavourable prognosis accompanied with resistance to radio- and chemo-therapy due to the emergence of androgen-independence[4]. It is urgent to develop novel agents that inhibit the proliferation and growth, and reverse the multidrug resistance and recurrence of CaP cells. It has been reported that T-96 exhibited anti-cancer

effect on various malignant carcinomas, including melanoma[24], glioblastoma[25], breast cancer[26] and pancreatic cancer [27].However, its cytotoxicity and molecular mechanisms against CaP have not been clearly explored. In the current study, we demonstrated that T-96 was a potent inhibitor of CaP through inducing cell cycle arrest at S-phase and extrinsic-apoptosis signalling pathway. Mechanism investigation indicated that through enhancing the levels of intracellular accumulation of ROS, T-96 significantly triggered ER stress, autophagy initiation while autophagic flux suppression and finally extrinsic apoptosis in CaP cells, implying that autophagic flux suppression induced by ER stress response after treatment with T-96 promoted caspase 8 dependent external-apoptosis to inhibit CaP cells. Meanwhile, our findings indicated that T-96 could act as a synergist to improve ciplatin-mediated cytotoxicity in CaP cells.

It has been reported that perturbations in ER functions induced by the change of tumor cell microenvironmentor the effects of anti-tumor drugs can trigger ER stress, leading to the accumulation of unfolded proteins in the ER lumen[41, 42].ROS overload is the most important inducer of ER stress in the cells[43]. ER stress has a dualistic role in tumour, to promote cell survival or trigger cell death. Actually, it was indicated that a slight UPR and ER stress act as an accommodative mechanism to promote cancerous cells to construct multiple antiapoptotic mechanisms for protecting cells from chemotherapy-mediated cell death, thus serving as a major factor in inducing chemotherapy drug resistance [44–46].Additionally, as mentioned before, the cancerous cells will be subjected to cell apoptosis when ER stress is so excessive or severe that it surpasses the protective capability of UPR[47, 46, 48].In accordance with that, along with high levels of ROS, we also found that T-96 treatment remarkably up-regulated the expression of the UPR hallmarks p-PERK, IRE1α, Ero1-L1α and PDI, and significantly increased intracellula $Ca^{2+}$ levels in CaP cells, suggesting the induction of ER stress under exposure to it.

In addition, ER stress is usually related to the initiation of autophagy during cellular physiological and pathological stress as well as during chemotherapy[49–52]. Autophagy is a vital dynamic and evolutionarily conserved process aimed to capture unnecessary or dysfunctional cellular components and form autophagolysosomes for degradation. Meanwhile, autophagy has a double-edged sword role in cancerous cells as it can either increase or decrease survival[53, 54]. Autophagy induction is mainly regulated by coordinated phosphorylation of serine/threonine kinase UNC-51-like kinase 1 (ULK1) phosphorylated by either AMPK or mTOR[55]. As expected, we found that a remarkable decrease in LC3I protein and p-mTOR (Ser2448) levels, and a dramatically increase in p-AMPK (Thr172) level in CaP cells after exposure to T-96, confirming the reported findings that autophagy induction may bealternatively regulated by AMPK and mTOR. However, some reports indicated that suppression of mTOR would rather block the autophagic flux, thus results in increased autophagosome accumulation rather than autophagy initiation[56, 57]. These findings support our findings that down-regulation of mTOR phosphorylation might be vital to T-96-induced autophagic flux impairment.

MAPK/ERK activation has been demonstrated to regulate various cell responses such as proliferation, migration and differentiation[58]. High levels of MAPK/ERK phosphorylation has been detected in many malignant tumors, but MAPK/ERK activation is not always involved in cell survival protection, it can also

interplay with cell death such as autophagy, apoptosis and senescence[58, 59]. However, the exact effect of MAPK/ERK on autophagy activation and maturation has not been defined and generates controversial results[35]. Increasing evidence demonstrates that prolonged activation of MAPK/ERK induced by drug treatment has been indicated to block the maturation process of autophagy[36, 37]. In consistent with these studies, our results indicated that both autophagy and ERK were activated while autophagic flux was impaired after treatment with T-96. We inferred that T-96-mediated ERK activation might be an inducer to play important role in autophagy initiation and autophagic flux blockage. Moreover, activation of MAPK/ERK has been reported to impair autophagy process by promoting the degradation of Fork head Box O1 (FOXO1) in cancer cells which is a protein associated with maintenance of autophagic flux in cancer cells[60, 61]. It will be interesting to evaluate whether the effect of T-96 on MPAK/ERK activation is mediated by targeting FOXO1 and how they transfer the ER stress signal to finally initiate autophagy and impair autophagic flux in CaP cells in our future study.

Recently, growing results have been indicated that autophagy induced by chemotherapy or radiotherapy may lead to generation of resistance whereas the impairment of autophagic flux can improve cells' sensitivity to chemotherapy due to cell death induction[38–40]. Thus, novel autophagy inhibitors are worthwhile to be explored for increasing the treatment efficacy of chemotherapeutic drugs towards cancer. In the current study, we found that T-96 enhanced the sensitivity of cisplatin in CaP cells through regulating autophagy induced by ER stress. Obviously, considering the certain anticancer activity of T-96, combination of T-96 with other chemotherapeutic drugs might be an effective manner for cancer therapy.

In conclusion, our study demonstrates that T-96 reduced CaP cell survival by inducing cell cycle arrest and apoptosis. The prolonged ER stress, which can regulate autophagy and activate apoptosis, might account for the underlying mechanisms of cell death caused by T-96 and its synergy effect with cisplatin on inhibition of CaP cells. Our findings suggest that T-96 is a specific ER stress and autophagy regulator and has the potential to be developed as an adjuvant for further cancer therapy, especially in CaP treatment.

# Declarations

Acknowledgments This research was funded by the Basic Research and Frontier Program of Chongqing Science and Technology Bureau (cstc2018jcyjAX0219, cstc2019jcyj-msxmX0727, cstc2020jcyj-msxmX0595, cstc2020jcyj-msxm2370 and cstc2020jcyj-msxmX0733), Science and Technology Research Program of Chongqing Municipal Education Commission (KJZD-K20200130, KJQN201901331 and KJQN201801304) and Scientific Research Foundation of the Chongqing University of Arts and Sciences (2017RBX11, Y2019XY19 and Y2020XY14).

Availability of data and material The datasets and materials obtained and analyzed during the current study were available from the corresponding authors in a reasonable request.

Compliance with ethical standards

Conflict of interest The authors declare that they have no conflict of interest.

# References


1. Martignano F, Rossi L, Maugeri A, Gallà V, Conteduca V, De Giorgi U, et al. Urinary RNA-based biomarkers for prostate cancer detection. Clin Chim Acta. 2017;473:96–105. doi:10.1016/j.cca.2017.08.009.
2. Dai C, Heemers H, Sharifi N. Androgen signaling in prostate cancer. Cold Spring Harb Perspect Med. 2017;7(9):a030452. doi:10.1101/cshperspect.a030452.
3. Yap TA, Smith AD, Ferraldeschi R, Al-Lazikani B, Workman P, De Bono JS. Drug discovery in advanced prostate cancer: translating biology into therapy. Nat Rev Drug Discov. 2016;15(10):699. doi:10.1038/nrd.2016.120.
4. Valerio M, Emberton M, Eggener SE, Ahmed HU. The challenging landscape of medical device approval in localized prostate cancer. Nat Rev Urol. 2016;13(2):91. doi:10.1038/nrurol.2015.289.
5. Fong ZV, Tanabe KK. The clinical management of hepatocellular carcinoma in the United States, Europe, and Asia: a comprehensive and evidence-based comparison and review. Cancer. 2014;120(18):2824–38. doi:10.1002/cncr.28730.
6. Anelli T, Sitia R. Protein quality control in the early secretory pathway. EMBO J. 2008;27(2):315–27. doi:10.1038/sj.emboj.7601974.
7. Tabas I, Ron D. Integrating the mechanisms of apoptosis induced by endoplasmic reticulum stress. Nat Cell Biol. 2011;13(3):184–90. doi:10.1038/ncb0311-184.
8. Jeong JS, Kim SR, Cho SH, Lee YC. Endoplasmic reticulum stress and allergic diseases. Curr Allergy Asthma Rep. 2017;17(12):82. doi:10.1007/s11882-017-0751-9.
9. Grootjans J, Kaser A, Kaufman RJ, Blumberg RS. The unfolded protein response in immunity and inflammation. Nat Rev Immunol. 2016;16(8):469. doi:10.1038/nri.2016.62.
10. Arensdorf A, Diedrichs D, Rutkowski T. Regulation of the transcriptome by ER stress: non-canonical mechanisms and physiological consequences. Front Genet. 2013;4:256. doi:10.3389/fgene.2013.00256.
11. Hetz C. The unfolded protein response: controlling cell fate decisions under ER stress and beyond. Nat Rev Mol Cell Biol. 2012;13(2):89–102. doi:10.1038/nrm3270.
12. Liu M-q, Chen Z, Chen L-x. Endoplasmic reticulum stress: a novel mechanism and therapeutic target for cardiovascular diseases. Acta Pharmacol Sin. 2016;37(4):425–43. doi:10.1038/aps.2015.145.
13. Dandekar A, Mendez R, Zhang K. Cross talk between ER stress, oxidative stress, and inflammation in health and disease. Methods Mol Biol. 2015:205–14. doi:10.1007/978-1-4939-2522-3_15.
14. Shore GC, Papa FR, Oakes SA. Signaling cell death from the endoplasmic reticulum stress response. Curr Opin Cell Biol. 2011;23(2):143–9. doi:10.1016/j.ceb.2010.11.003.
15. Tao X, Younger J, Fan FZ, Wang B, Lipsky PE. Benefit of an extract of Tripterygium Wilfordii Hook F in patients with rheumatoid arthritis: A double-blind, placebo-controlled study. Arthritis Rheum.

2002;46(7):1735–43. doi:10.1002/art.10411.

16. Ji W, Li J, Lin Y, Song Y-n, Zhang M, Ke Y, et al. Report of 12 cases of ankylosing spondylitis patients treated with Tripterygium wilfordii. Clin Rheumatol. 2010;29(9):1067–72. doi:10.1007/s10067-010-1497-0.
17. Tao X, Fan F, Hoffmann V, Gao CY, Longo NS, Zerfas P, et al. Effective therapy for nephritis in (NZB× NZW) F1 mice with triptolide and tripdiolide, the principal active components of the Chinese herbal remedy Tripterygium wilfordii Hook F. Arthritis Rheum. 2008;58(6):1774–83. doi:10.1002/art.23513.
18. Han R, Rostami-Yazdi M, Gerdes S, Mrowietz U. Triptolide in the treatment of psoriasis and other immune-mediated inflammatory diseases. Br J Clin Pharmacol. 2012;74(3):424–36. doi:10.1111/j.1365-2125.2012.04221.x.
19. Luo D, Zhao J, Rong J. Plant-derived triterpene celastrol ameliorates oxygen glucose deprivation-induced disruption of endothelial barrier assembly via inducing tight junction proteins. Phytomedicine. 2016;23(13):1621–8. doi:10.1016/j.phymed.2016.10.006.
20. Mujumdar N, Mackenzie TN, Dudeja V, Chugh R, Antonoff MB, Borja–Cacho D, et al. Triptolide induces cell death in pancreatic cancer cells by apoptotic and autophagic pathways. Gastroenterology. 2010;139(2):598–608. doi:10.1053/j.gastro.2010.04.046.
21. Oliveira AR, Beyer G, Chugh R, Skube SJ, Majumder K, Banerjee S, et al. Triptolide abrogates growth of colon cancer and induces cell cycle arrest by inhibiting transcriptional activation of E2F. Lab Invest. 2015;95(6):648–59. doi:10.1038/labinvest.2015.46.
22. Zhao X, Gao S, Ren H, Huang H, Ji W, Hao J. Inhibition of autophagy strengthens celastrol-induced apoptosis in human pancreatic cancer in vitro and in vivo models. Curr Mol Med. 2014;14(4):555–63. doi:10.2174/1566524014666140414211223.
23. Xu W, Lin Z, Yang C, Zhang Y, Wang G, Xu X, et al. Immunosuppressive effects of demethylzeylasteral in a rat kidney transplantation model. Int Immunopharmacol. 2009;9(7–8):996–1001. doi:10.1016/j.intimp.2009.04.007.
24. Zhao Y, He J, Li J, Peng X, Wang X, Dong Z, et al. Demethylzeylasteral inhibits cell proliferation and induces apoptosis through suppressing MCL1 in melanoma cells. Cell Death Dis. 2017;8(10):e3133-e. doi:10.1038/cddis.2017.529.
25. Zhang K, Fu G, Pan G, Li C, Shen L, Hu R, et al. Demethylzeylasteral inhibits glioma growth by regulating the miR-30e-5p/MYBL2 axis. Cell Death Dis. 2018;9(10):1–14. doi:10.1038/s41419-018-1086-8.
26. Li L, Ji Y, Fan J, Li F, Li Y, Wu M, et al. Demethylzeylasteral (T-96) inhibits triple-negative breast cancer invasion by blocking the canonical and non-canonical TGF-β signaling pathways. Naunyn Schmiedebergs Arch Pharmacol. 2019;392(5):593–603. doi:10.1007/s00210-019-01614-5.
27. Wang F, Tian X, Zhang Z, Ma Y, Xie X, Liang J, et al. Demethylzeylasteral (ZST 93) inhibits cell growth and enhances cell chemosensitivity to gemcitabine in human pancreatic cancer cells via apoptotic and autophagic pathways. Int J Cancer. 2018;142(9):1938–51. doi:10.1002/ijc.31211.

28. Shen M, Wang L, Wang B, Wang T, Yang G, Shen L, et al. Activation of volume-sensitive outwardly rectifying chloride channel by ROS contributes to ER stress and cardiac contractile dysfunction: involvement of CHOP through Wnt. Cell Death Dis. 2014;5(11):e1528-e. doi:10.1038/cddis.2014.479.
29. Chen Y, Liu JM, Xiong XX, Qiu XY, Pan F, Liu D, et al. Piperlongumine selectively kills hepatocellular carcinoma cells and preferentially inhibits their invasion via ROS-ER-MAPKs-CHOP. Oncotarget. 2015;6(8):6406. doi:10.18632/oncotarget.3444.
30. Hasanain M, Bhattacharjee A, Pandey P, Ashraf R, Singh N, Sharma S, et al. α-Solanine induces ROS-mediated autophagy through activation of endoplasmic reticulum stress and inhibition of Akt/mTOR pathway. Cell Death Dis. 2015;6(8):e1860. doi:10.1038/cddis.2015.219.
31. Liao C, Zheng K, Li Y, Xu H, Kang Q, Fan L, et al. Gypenoside L inhibits autophagic flux and induces cell death in human esophageal cancer cells through endoplasm reticulum stress-mediated Ca2 + release. Oncotarget. 2016;7(30):47387. doi:10.18632/oncotarget.10159.
32. Krebs J, Agellon LB, Michalak M. Ca2 + homeostasis and endoplasmic reticulum (ER) stress: An integrated view of calcium signaling. Biochem Biophys Res Commun. 2015;460(1):114–21. doi:10.1016/j.bbrc.2015.02.004.
33. Yorimitsu T, Nair U, Yang Z, Klionsky DJ. Endoplasmic reticulum stress triggers autophagy. J Biol Chem. 2006;281(40):30299–304. doi:10.1074/jbc.M607007200.
34. Dikic I, Elazar Z. Mechanism and medical implications of mammalian autophagy. Nat Rev Mol Cell Biol. 2018;19(6):349–64. doi:10.1038/s41580-018-0003-4.
35. Sridharan S, Jain K, Basu A. Regulation of autophagy by kinases. Cancers. 2011;3(2):2630–54. doi:10.3390/cancers3022630.
36. Corcelle E, Nebout M, Bekri S, Gauthier N, Hofman P, Poujeol P, et al. Disruption of autophagy at the maturation step by the carcinogen Lindane is associated with the sustained mitogen-activated protein kinase/extracellular signal–regulated kinase activity. Cancer Res. 2006;66(13):6861–70. doi:10.1158/0008-5472.CAN-05-3557.
37. Kuo H-H, Kakadiya R, Wu Y-C, Su T-L, Lee T-C, Lin Y-W, et al. Derivatives of 6-cinnamamido-quinoline-4-carboxamide impair lysosome function and induce apoptosis. Oncotarget. 2016;7(25):38078. doi:10.18632/oncotarget.9348.
38. Yang C, Wu C, Xu D, Wang M, Xia Q. AstragalosideII inhibits autophagic flux and enhance chemosensitivity of cisplatin in human cancer cells. Biomed Pharmacother. 2016;81:166–75. doi:10.1016/j.biopha.2016.03.025.
39. Wen Z-p, Zeng W-j, Chen Y-h, Li H, Wang J-y, Cheng Q, et al. Knockdown ATG4C inhibits gliomas progression and promotes temozolomide chemosensitivity by suppressing autophagic flux. J Exp Clin Cancer Res. 2019;38(1):298. doi:10.1186/s13046-019-1287-8.
40. Zhang X, Kumstel S, Jiang K, Meng S, Gong P, Vollmar B, et al. LW6 enhances chemosensitivity to gemcitabine and inhibits autophagic flux in pancreatic cancer. J Adv Res. 2019;20:9–21. doi:10.1016/j.jare.2019.04.006.
41. Perlmutter DH. Misfolded proteins in the endoplasmic reticulum. Lab Invest. 1999;79(6):623–38.

42. Ruiz A, Matute C, Alberdi E. Intracellular Ca 2 + release through ryanodine receptors contributes to AMPA receptor-mediated mitochondrial dysfunction and ER stress in oligodendrocytes. Cell Death Dis. 2010;1(7):e54-e. doi:10.1038/cddis.2010.31.
43. Kim I, Xu W, Reed JC. Cell death and endoplasmic reticulum stress: disease relevance and therapeutic opportunities. Nat Rev Drug Discov. 2008;7(12):1013–30. doi:10.1038/nrd2755.
44. Brown JM, Giaccia AJ. The unique physiology of solid tumors: opportunities (and problems) for cancer therapy. Cancer Res. 1998;58(7):1408-16. doi: Published April 1998.
45. Moenner M, Pluquet O, Bouchecareilh M, Chevet E. Integrated endoplasmic reticulum stress responses in cancer. Cancer Res. 2007;67(22):10631–4. doi:10.1158/0008-5472.CAN-07-1705.
46. Wang W-A, Groenendyk J, Michalak M. Endoplasmic reticulum stress associated responses in cancer. Biochim Biophys Acta. 2014;1843(10):2143–9. doi:10.1016/j.bbamcr.2014.01.012.
47. Martinon F. Targeting endoplasmic reticulum signaling pathways in cancer. Acta Oncol. 2012;51(7):822–30. doi:10.3109/0284186X.2012.689113.
48. Yadav RK, Chae S-W, Kim H-R, Chae HJ. Endoplasmic reticulum stress and cancer. J Cancer Prev. 2014;19(2):75. doi:10.15430/JCP.2014.19.2.75.
49. Kouroku Y, Fujita E, Tanida I, Ueno T, Isoai A, Kumagai H, et al. ER stress (PERK/eIF2 α phosphorylation) mediates the polyglutamine-induced LC3 conversion, an essential step for autophagy formation. Cell Death Differ. 2007;14(2):230–9. doi:10.1038/sj.cdd.4401984.
50. Maiuri MC, Zalckvar E, Kimchi A, Kroemer G. Self-eating and self-killing: crosstalk between autophagy and apoptosis. Nat Rev Mol Cell Biol. 2007;8(9):741–52. doi:10.1038/nrm2239.
51. Xu L, Liu J-H, Zhang J, Zhang N, Wang Z-H. Blockade of autophagy aggravates endoplasmic reticulum stress and improves Paclitaxel cytotoxicity in human cervical cancer cells. Cancer Res Treat. 2015;47(2):313. doi:10.4143/crt.2013.222.
52. Huang K, Chen Y, Zhang R, Wu Y, Ma Y, Fang X, et al. Honokiol induces apoptosis and autophagy via the ROS/ERK1/2 signaling pathway in human osteosarcoma cells in vitro and in vivo. Cell Death Dis. 2018;9(2):1–17. doi:10.1038/s41419-017-0166-5.
53. Bel S, Hooper LV. Secretory autophagy of lysozyme in Paneth cells. Autophagy. 2018;14(4):719–21. doi:10.1080/15548627.2018.1430462.
54. Cheng X, Feng H, Wu H, Jin Z, Shen X, Kuang J, et al. Targeting autophagy enhances apatinib-induced apoptosis via endoplasmic reticulum stress for human colorectal cancer. Cancer Lett. 2018;431:105–14. doi:10.1016/j.canlet.2018.05.046.
55. Kim J, Kundu M, Viollet B, Guan K-L. AMPK and mTOR regulate autophagy through direct phosphorylation of Ulk1. Nat Cell Biol. 2011;13(2):132–41. doi:10.1038/ncb2152.
56. Cinà DP, Onay T, Paltoo A, Li C, Maezawa Y, De Arteaga J, et al. Inhibition of MTOR disrupts autophagic flux in podocytes. J Am Soc Nephrol. 2012;23(3):412–20. doi:10.1681/ASN.2011070690.

57. Button RW, Vincent JH, Strang CJ, Luo S. Dual PI-3 kinase/mTOR inhibition impairs autophagy flux and induces cell death independent of apoptosis and necroptosis. Oncotarget. 2016;7(5):5157. doi:10.18632/oncotarget.6986.
58. Mebratu Y, Tesfaigzi Y. How. ERK1/2 activation controls cell proliferation and cell death: Is subcellular localization the answer? Cell cycle. 2009;8(8):1168–75. doi:10.4161/cc.8.8.8147.
59. Cagnol S, Chambard JC. ERK and cell death: mechanisms of ERK-induced cell death–apoptosis, autophagy and senescence. FEBS J. 2010;277(1):2–21. doi:10.1111/j.1742-4658.2009.07366.x.
60. Zhao Y, Li X, Ma K, Yang J, Zhou J, Fu W, et al. The axis of MAPK1/3-XBP1u-FOXO1 controls autophagic dynamics in cancer cells. Autophagy. 2013;9(5):794–6. doi:10.4161/auto.23918.
61. He W, Zhang A, Qi L, Na C, Jiang R, Fan Z, et al. FOXO1, a potential therapeutic target, regulates autophagic flux, oxidative stress, mitochondrial dysfunction, and apoptosis in human cholangiocarcinoma QBC939 cells. Cell Physiol Biochem. 2018;45(4):1506–14. doi:10.1159/000487576.

# Figures

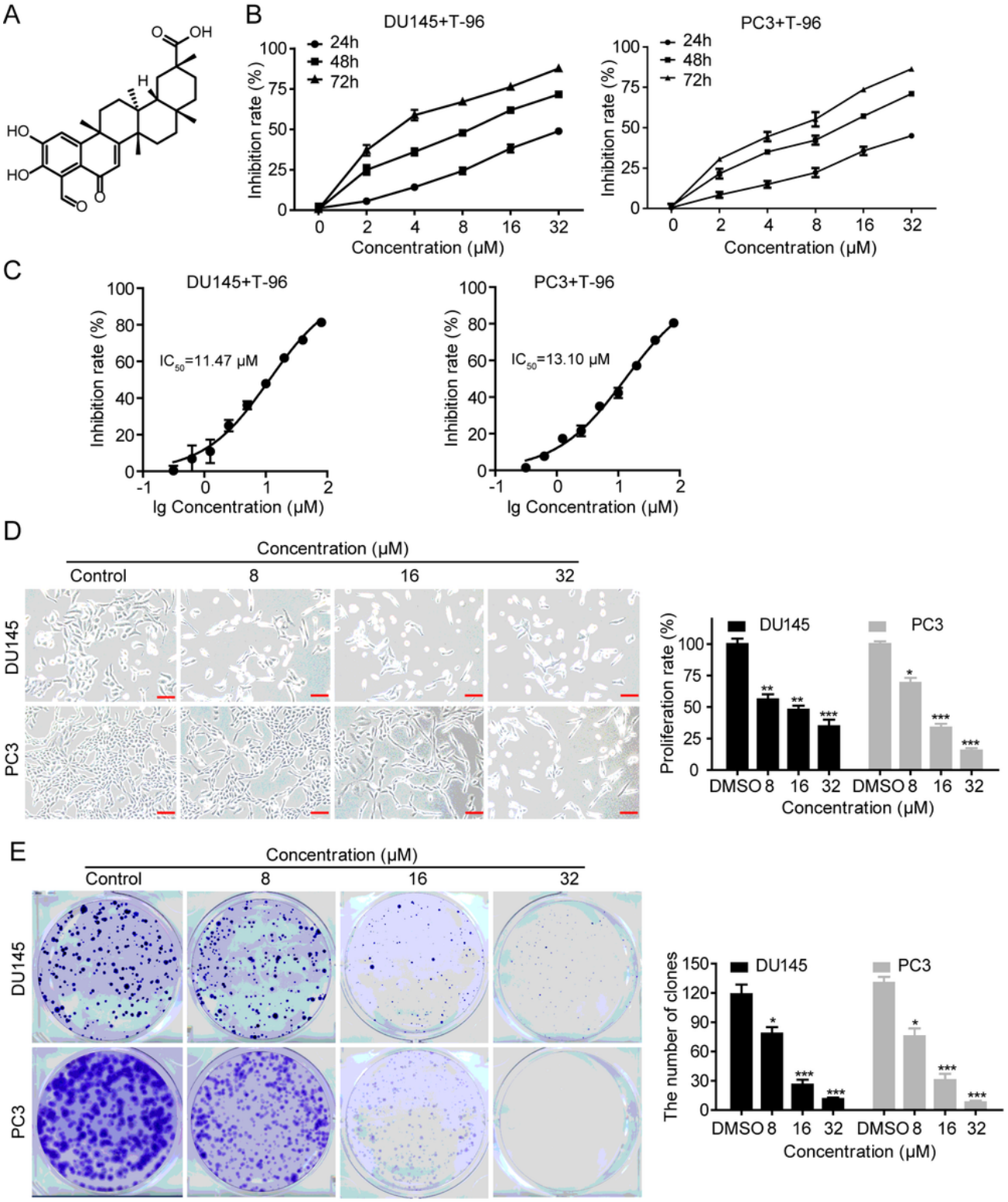


## Figure 1

The anti-proliferative effect of T-96 on human CaP lines. (A) The chemical structure of T-96. (B) The inhibition rates of T-96 on DU145 and PC3 cells. Both DU145 and PC3 cells were exposed to indicated concentrations of T-96 for 24, 48 and 72 h. MTT was performed to measure cell viability and growth. (C) IC50 values of T-96 in DU145 and PC3 cells were calculated. (D) Cell morphology of DU145 and PC3cells was captured with microscope after treatment with vehicle (0.05% DMSO) or the indicated concentrations

of T-96 for 48 h. Scale bar, 100 μm. The histogram showed the quantification of cell proliferation rate. (E) Colony formation assay was used to evaluate the in vitro growth of both DU145 and PC3 cells after exposure to the indicated doses of T-96 for 7 days. The colonies were visualized with the images and quantitated by histogram. All data were demonstrated as the mean ± SD of three independent experiments. *P < 0.05; **P < 0.01 versus vehicle.

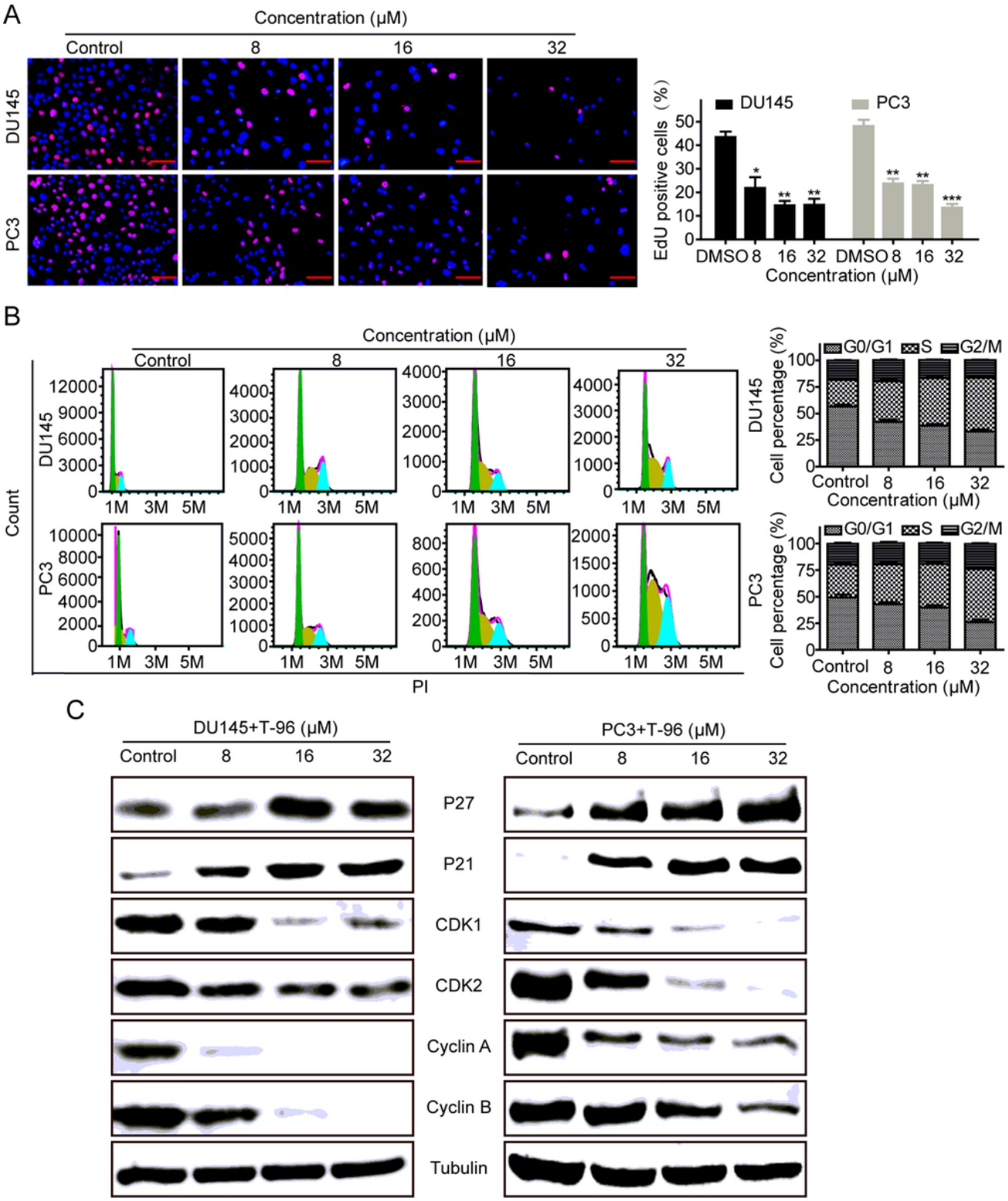


Figure 2

T-96 induced cell cycle at S phase to exhibit anticancer effect. (A) T-96 suppressed the CaP cell proliferation. EdU-staining assay was conducted to access the inhibition of cell proliferation after treatment with T-96 for 48 h. Scale bar, 100 μm. (B) The cell cycle of DU145 and PC3 cells was measured by flow cytometry in the presence of vehicle or T-96, and the percentages of cell population in different periods were quantitated with three independent experiments. (C) Effects of T-96 on the expression levels of S-phase related proteins in DU145 and PC3 cells were examined by western blotting after exposure to T-96 for 48 h.β-tubulin was used as a loading control. All data were demonstrated as the mean ± SD of three independent experiments. "*" represents $P < 0.05$; "**" represents $P < 0.01$; "***" represents $P < 0.001$.

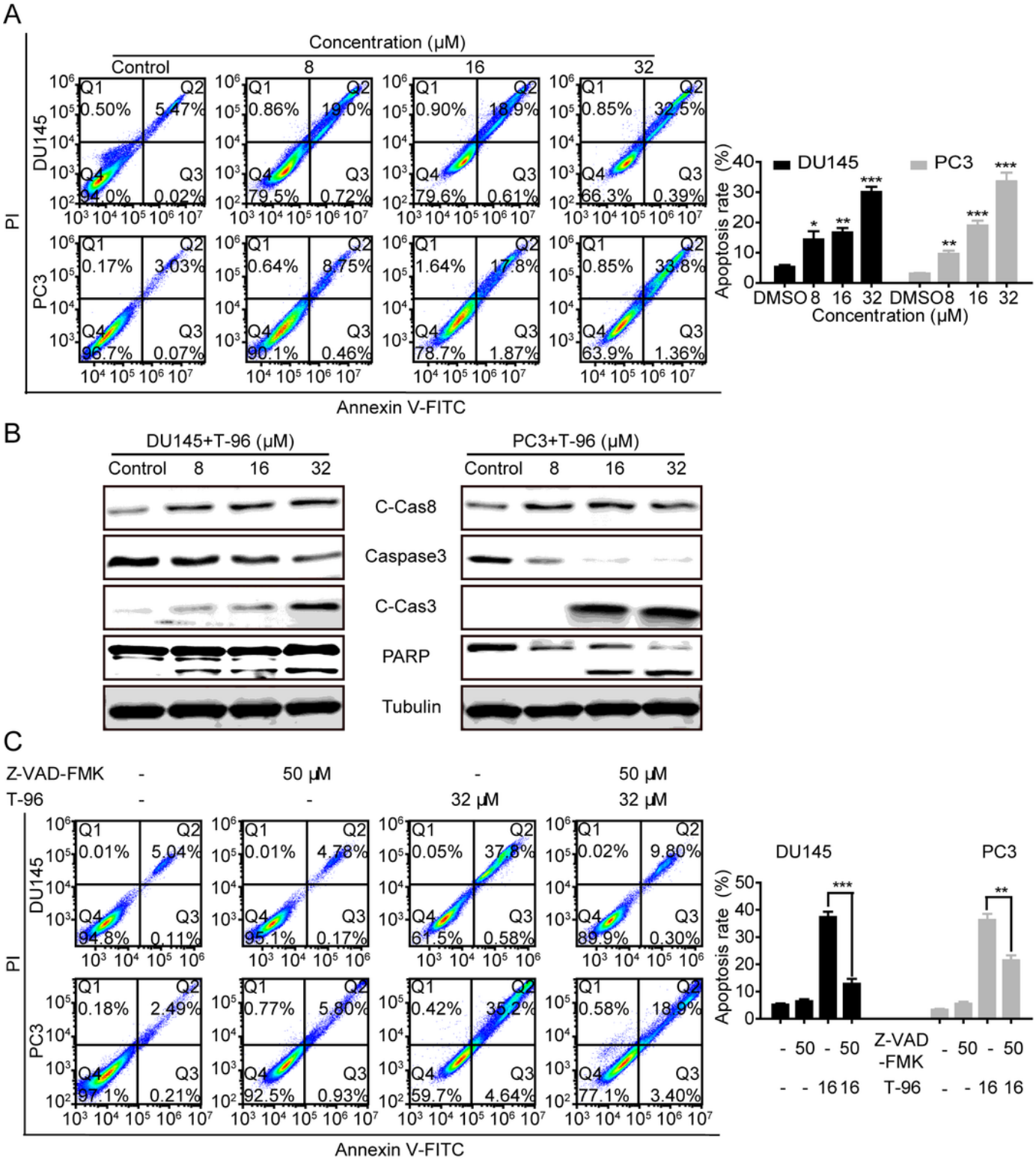


## Figure 3

T-96induced caspase-3-dependent apoptotic cell death in human CaP cells. (A and C) Apoptotic cell death in DU145 and PC3 cells were measured by flow cytometry after treatment with or without T-96, Z-VAD-FMK (50 μM), T-96 and Z-VAD-FMK (50 μM) for 48 h. (B) The expression of indicated proteins in DU145 and PC3 cells were examined by western blotting after exposure to T-96 for 48 h. β-tubulin was loaded as

a control. Data represent the mean ± SD of three independent experiments. *p<0.05, **p<0.01 and ***p<0.001.

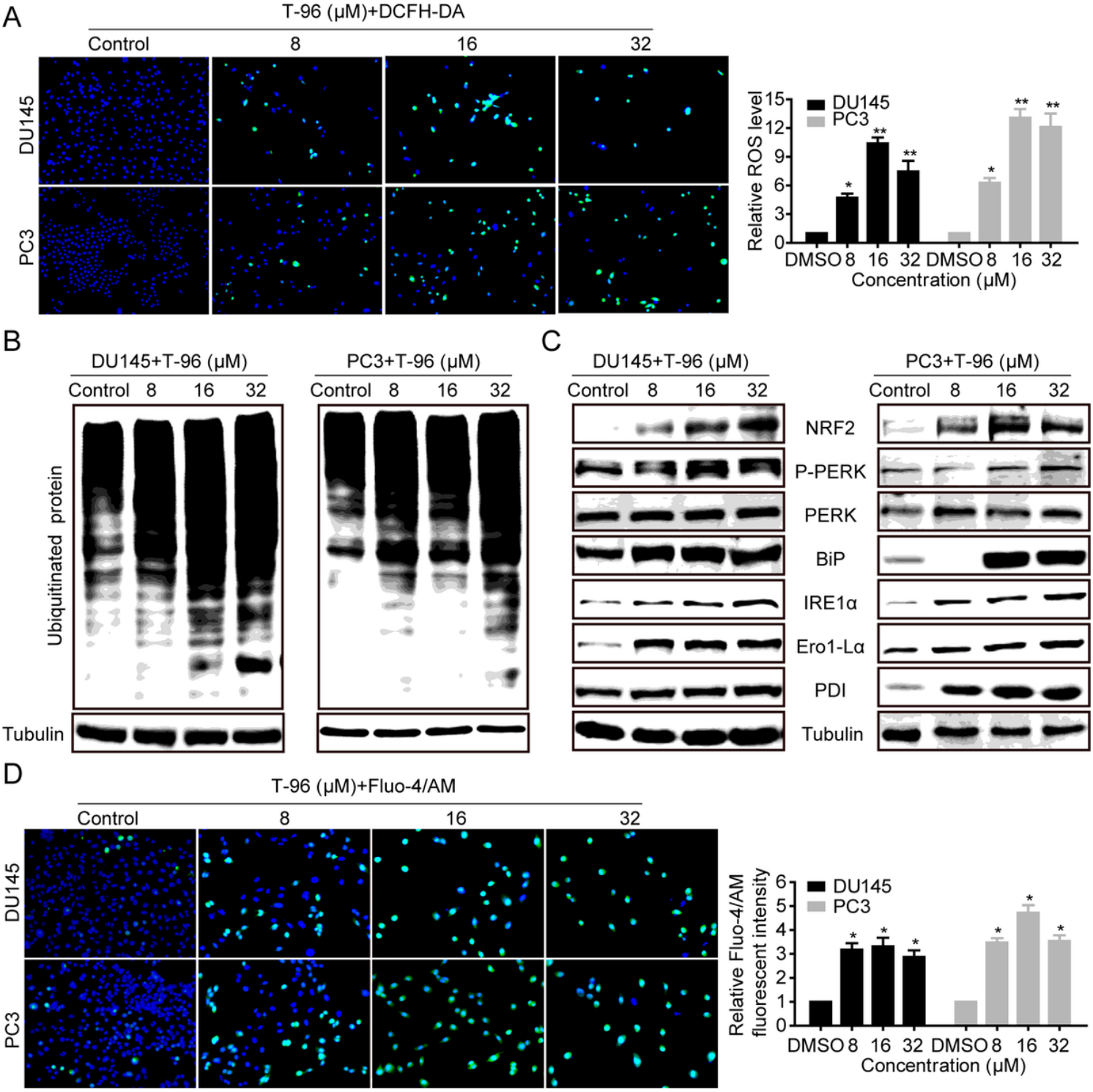


Figure 4

T-96-mediatedROS accumulation induced ER stress. (A) DU145 and PC3 cells were exposed to the indicated concentrations ofT-96 for 48 h, and then treated with DCFH-DA for another 30 min. Immunofluorescence analysis was performed to examine the green signal representing ROS generation. Green signal cells were counted and presented in the histogram. Scale bar: 100 μm. (B) T-96 induced

accumulation of ubiquitinated proteins. DU145 and PC3 cellswere treated with indicated concentrations of T-96 for 48 h, and the ubiquitination levels then were detected using western blotting. (C) T-96 activated the UPR pathway in a dose dependent manner. UPR pathway-related proteins were detected using western blotting. (D) T-96 enhanced intracellular Ca2+ concentration in a dose dependent manner. DU145 and PC3 cells were exposed to the indicated concentrations of T-96 for 24 h, and then cells were incubated with 5 μM Fluo-4/AM for 1 h and detected by fluorescence microscopy. Data are presented as the means ± SD. *p<0.05 and **p<0.01 compared with the control group.

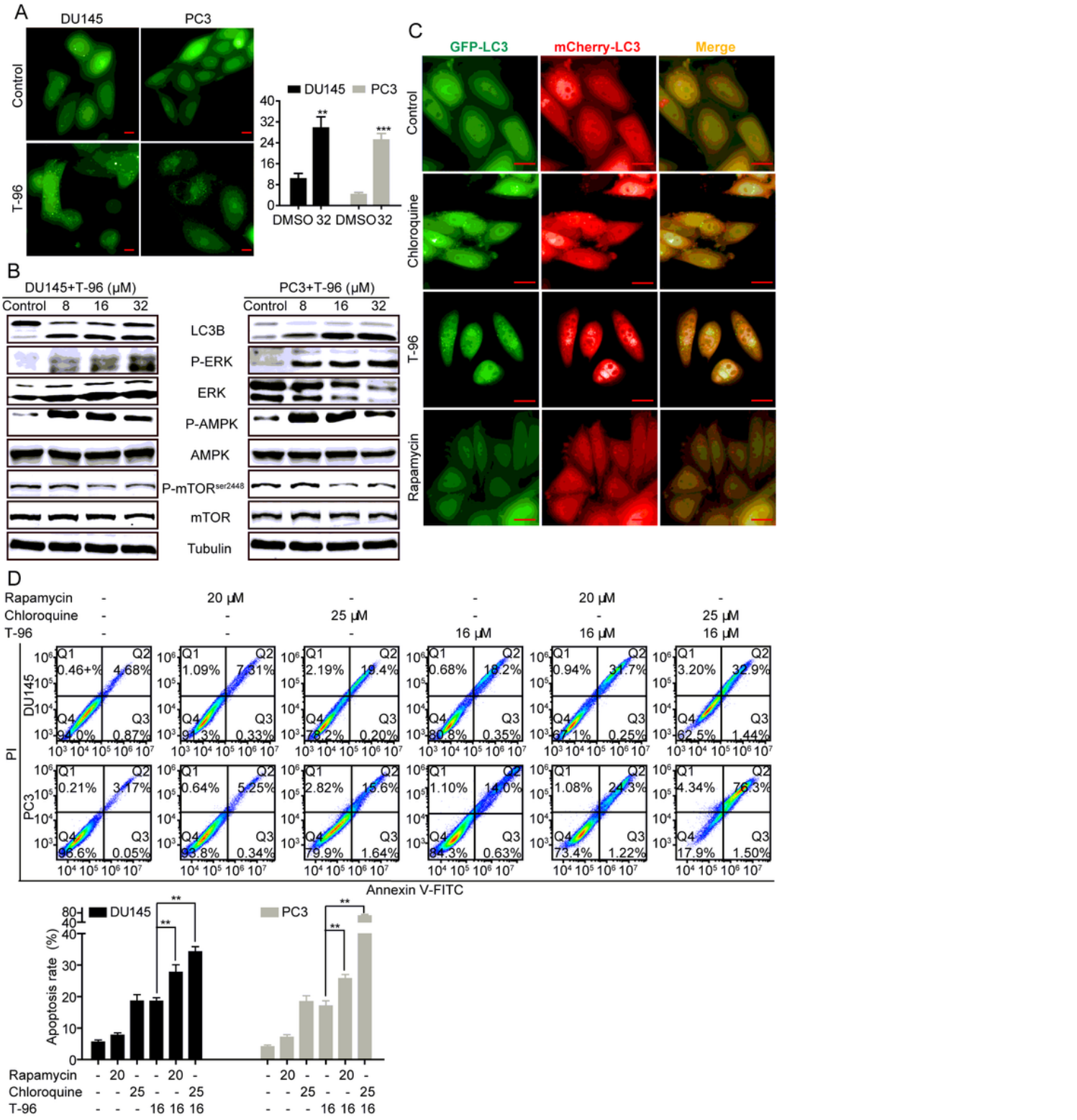

Figure 5

T-96 initiated autophagy while blocked autophagic flux in human CRC cells. (A) The punctate staining pattern of LC3 was detected using high content analysis system-operetta CLSTM in DU145 and PC3 cells after treatment with increasing concentrations of T-96 for 48 h. Scale bar, 10μm. (B) The protein expression levels involved in autophagy initiation were detected after exposure to T-96 using western blotting. β-tubulin was used as a loading control. (C) T-96 suppressed the autophagic flux in PC3 cells overexpressing mCherry-EGFP-LC3. Both cells were treated with indicated concentrations of T-96 for 24 h and then observed with fluorescent microscopy. Scale bar, 10 μm. Quantitative analysis of the autophagosome accumulation in T-96-treated cells. Yellow dots representing the autophagosomes were counted in three independent experiments. Red fluorescent labeled autophagolysosomes. (D) Autophagic flux suppression significantly increased apoptosis. Both DU145 and PC3 cell lines were treated with or without rapamycin, chloroquine, T-96, rapamycin and T-96, chloroquine and T-96, respectively. Then, apoptosis rate was measured using flow cytometry. Data represent the mean ± SD of three independent experiments. **p<0.01 and ***p<0.001compared with the control group.

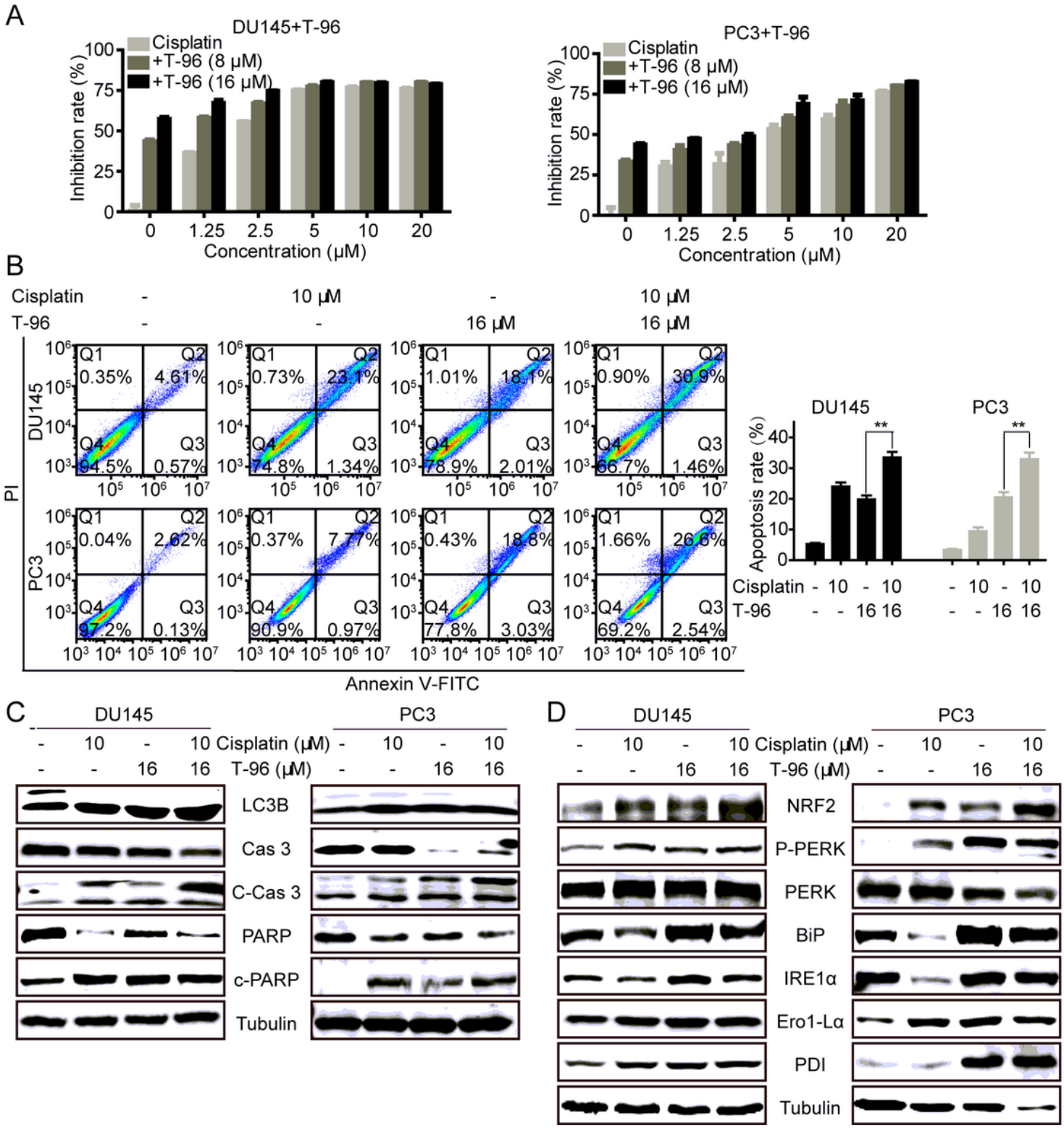


Figure 6

T-96 enhanced sensitivity to cisplatinin human CaP cells. (A) T-96 increased the cytotoxicity of cisplatin to CaP cells. Both DU145 and PC3 cells were treated with indicated concentrations of T-96 and cisplatin for 48 h. MTT was conducted to detect the effect of T-96 on the cytotoxicity of cisplatin to CaP cells. (B and C) Combined treatment of T-96 and cisplatin caused a higher apoptotic rate than that of monotherapy. DU145 and PC3 cells were treated with or without T-96, cisplatin, T-96 and cisplatin for 48

h, and then the apoptotic cell death was measured by flow cytometry. Meanwhile, the expression levels of indicated proteins were detected using western blotting. (D) Co-treatment with T-96 and cisplatin was more effective in initiating oxidative stress response and UPR. Western blotting was used to examine NRF2 and the UPR associated proteins after treatment with or wihout T-96 and cisplatin. β-tubulin was used as a loading control. Data represent the mean ± SD of three independent experiments. **p<0.01 compared with the control group.